Marine Environmental Research 188 (2023) 105976

Contents lists available at ScienceDirect

Marine Environmental Research

journal homepage: www.elsevier.com/locate/marenvrev

Mesozooplankton size structure in the Canary Current System

María Couret [a,*], José M. Landeira [a], Víctor M. Tuset [a], Airam N. Sarmiento-Lezcano [a], Pedro Vélez-Belchí [b], Santiago Hernández-León [a]

[a] Instituto de Oceanografía y Cambio Global, IOCAG, Universidad de Las Palmas de Gran Canaria, Unidad Asociada ULPGC-CSIC, Campus de Taliarte, 35214, Telde, Gran Canaria, Canary Islands, Spain
[b] Instituto Español de Oceanografía, CO Canarias, Santa Cruz de Tenerife, Spain

ARTICLE INFO

Keywords:
Mesozooplankton
Size spectra
Abundance distribution
Community structure
Canaries-African transition zone

ABSTRACT

Changes in plankton composition influences the dynamics of marine food webs and carbon sinking rates. Understanding the core structure and function of the plankton distribution is of paramount importance to know their role in trophic transfer and efficiency. Here, we studied the zooplankton distribution, abundance, composition, and size spectra for the characterization of the community under different oceanographic conditions in the Canaries-African Transition Zone (C-ATZ). This region is a transition zone between the coastal upwelling and the open ocean showing a high variability because of the physical, chemical, and biological changes between eutrophic and oligotrophic conditions through the annual cycle. During the late winter bloom (LWB), chlorophyll *a* and primary production were higher compared to that of the stratified season (SS), especially in the upwelling influenced area. Abundance distribution analysis clustered stations into two main groups according to the season (productive *versus* stratified season), and one group sampled in the upwelling influenced area. Size-spectra analysis showed steeper slopes during daytime in the SS, suggesting a less structured community and a higher trophic efficiency during the LWB due to the favorable oceanographic conditions. We also observed a significant difference between day and nighttime size spectra due to community change during diel vertical migration. Cladocera were the key taxa differentiating an Upwelling-group, from a LWB- and SS-group. These two latter groups were differentiated by Salpidae and Appendicularia mainly. Data obtained in this study suggested that abundance composition might be useful when describing community taxonomic changes, while size-spectra gives an idea of the ecosystem structure, predatory interactions with higher trophic levels and shifts in size structure.

1. Introduction

The determination of zooplankton community characteristics such as the abundance, biovolume, and size spectra has a great importance in biogeochemical cycles, energy flow, and vertical particle flux (Buitenhuis et al., 2010; Kiørboe, 2013; Noji, 1991). Zooplankton is widely used as bioindicators for the identification of shifts in phenology (Mackas et al., 2012), physiological rates (Lenz et al., 2021), upwelling strength (Oksana and Viacheslav, 2012), atmospheric forcing (Hooff and Peterson, 2006), and latitudinal displacement of species (Berraho et al., 2015). It has a large influence on abundance and distribution of fishery resources, especially pelagic species (Shi et al., 2020).

Spatial and temporal changes in zooplankton community structure and distribution pattern are important for understanding the core structure and function of marine ecosystems (Zhao et al., 2022), and the potential impacts of climate change (Batchelder et al., 2013; Hays et al., 2005; Shi et al., 2020). In addition, body size is one of the primary determinants of energy flow, species diversity, and population crowding (Peters and Wassenberg, 1983; Woodward et al., 2005). Size shapes the community structure as marine food-webs are size-structured, constraining prey-predator interactions and physiology (Li et al., 2018), and influences biomass and growth rates of populations in adjacent trophic levels (Carpenter et al., 1987; Vanni and Findlay, 1990). This parameter is used as a scaling factor and aggregation criterion to produce a macroscopic description of the pelagic ecosystems, with the objective of improving the predictive capacity of global models in anticipation of future responses of oceanic ecosystems to climate change (Stemmann and Boss, 2012). In this context, a method widely used for characterizing zooplankton is the normalized biomass size spectra (NBSS) (San Martin et al., 2006; Sprules and Munawar, 1986). The most frequently

* Corresponding author.
E-mail address: maria.couret@ulpgc.es (M. Couret).

https://doi.org/10.1016/j.marenvres.2023.105976
Received 2 December 2022; Received in revised form 21 March 2023; Accepted 4 April 2023
Available online 10 April 2023

employed model was that of Platt and Denman (1977, 1978), who introduced a theoretical concept considering the biomass flux as a continuous energy flow. Quantitative empirical analyses of planktonic structure are usually based on the parameters generated by the straight line fitted to the size spectrum. The slope mirrors the overall trend in biomass distribution among various size classes, the linear fit (r^2) reflects the stability of community structure, and the NBSS intercept is related to the total abundance of the system (San Martin et al., 2006), and to the level of primary production (Dai et al., 2016; García-Comas et al., 2014). The theory suggests that the NBSS slope of a pelagic steady-state community, where biomass is evenly distributed over logarithmic size classes, will be −1 (Sheldon et al., 1972). However, empirical studies have demonstrated that the NBSS slopes do not follow linearity in non-equilibrated highly dynamic ecosystems (García-Comas et al., 2014; Quinones et al., 2003). Several factors influence the NBSS slopes, highlighting sampling location and season (Krupica, 2006), sample processing method (e.g., Optical Plankton Counter or ZooScan) (Naito et al., 2019; Vandromme et al., 2012), productivity gradient (Kwong et al., 2022), nutrient stress (Atkinson et al., 2021; Wang et al., 2020), mesoscale structures (Chen et al., 2020; Jagadeesan et al., 2020), ecological processes (Zhou et al., 2014; Zhou, 2006), water depth gradient (Dai et al., 2017), oligotrophy (García-Comas et al., 2014), inter alia. Even NBSS slopes are highly sensible to environmental conditions and depend on many factors, they have been widely used as a metric of size structure (Zhou, 2006). Thus, the normalization of the biomass size spectrum allowed comparison across systems and was found to be a useful tool to assess simple first-order system dynamics (Heath, 1995). Even so, all studies recognize that plankton size distribution leads to general improvements in the description and dynamics of zooplankton and dead particle models in the mesopelagic layers (Stemmann and Boss, 2012). It might also be a more effective approach when comparing aquatic communities (Cottingham, 1999; Cózar et al., 2003), and useful to evaluate resource availability and selective predation on zooplankton (Braun et al., 2021).

The Canaries-African Transition Zone (C-ATZ) is part of the Canary Current System (CCS) and it is located within the eastern boundary gyre of the North Atlantic Ocean, also holding the upwelling system off Northwest Africa (NWA). This region is a transition zone between the coastal upwelling and the open ocean showing a high variability because of the physical, chemical, and biological changes between eutrophic and oligotrophic conditions (Barton et al., 1998; Hernández-León et al., 2007). Comparison of communities that are distant in latitude but connected by similar hydrological, chemical, and environmental conditions offers an opportunity to identify the influence of biogeography and environmental conditions on the types of organisms that inhabit them (Boucher, 1982). Upwelling areas are advantageous environments for this approach, with a small number of abundant species having similar importance in every region (Berraho et al., 2015). The NWA upwelling system is under a permanent upwelling regime characterized by coastal sea surface temperatures colder than the oceanic ones at the same latitude. North of 21°N, upwelling-favorable conditions occur from April to September, with a maximum in July, and less upwelling-favorable conditions from October to March, with a minimum in December to January (Gómez-Gesteira et al., 2008). Seasonal changes and upwelling strength also show a close link with the production of phytoplankton and zooplankton. In particular, zooplankton follows a strong annual cycle of biomass, productivity, and development sequence (Bertram et al., 2001). In the open ocean, primary production varies within the annual cycle, controlled by the nutrient enrichment during the so-called Late Winter Bloom (LWB). Organisms burst due to convective mixing during winter (Armengol et al., 2019; Neuer et al., 2007) eroding the thermocline (Cianca et al., 2007; Schmoker et al., 2012) and promoting a slight increase in nutrients in the euphotic zone. In spring, the seasonal thermocline is reestablished, remaining through the summer and autumn, restricting the injection of nutrients into the euphotic zone, and therefore limiting primary production (Schmoker et al., 2012).

The C-ATZ was mainly studied during different periods in relation to the effect of upwelling filaments and eddies (Barton et al., 1998) on phytoplankton (Arístegui et al., 2004), zooplankton (Hernández-León et al., 2002a), and fish and invertebrate larvae (Landeira et al., 2017; Rodríguez et al., 1999). There were large differences in productivity and plankton biomass between the oligo-, meso-, and eutrophic areas of the CCS during the annual cycle (Hernández-León et al., 2007), but no studies analyzed the spatial and temporal variability and seasonality in the region. Therefore, the aims of the present study were (i) to describe the seasonal effect (i.e., Late Winter Bloom, LWB *versus* Stratified Season, SS) in the zooplankton (i.e., species richness, abundance, and biomass) of two adjacent dynamic systems as the Canary Islands and the African platform, and (ii) to examine zooplankton responses using size spectra as a stational and spatial ecological indicator of their structure. Given the seasonal and spatial fluctuations zooplankton biomass occurring in the transition zone from the coast to the ocean (Hernández-León et al., 2002a, 2002b; Yebra et al., 2005) we hypothesize that the NBSS slope in the C-ATZ should be steeper in oligotrophic areas and flatter in areas with high productivity, highly depending on the abundance of organisms.

2. Material and methods

2.1. Field sampling

Zooplankton was collected during two cruises conducted from 21st to 29th October in 2018 (SS) and from 28th February to 9th March in 2019 (LWB) on board the R.V. Ángeles Alvariño. Sailing took place from the northwest of La Palma Island (Canary Islands) to the Western Sahara coast (NWA) (Fig. 1). Mesozooplankton samples were collected during either day or night using a double WP-2 net (UNESCO, 1968) equipped with a 200 μm mesh size. Tows were performed from 200 m depth to the surface with a vertical speed of 0.67 m s^{-1}. One of the samples from the double net was directly fixed on board with 4% formalin-seawater for later taxonomic studies, and the second sample was used for measuring biomass from protein content. The latter sample was sieved and size fractionated into 200, 500, and 1000 μm, frozen in liquid nitrogen, and stored at −80 °C until later analysis.

Vertical profiles of temperature, salinity, and chlorophyll *a* (Chl *a*) were obtained using a CTD (Seabird 911plus) mounted on a General Oceanic rosette sampler. The system was equipped with a chlorophyll

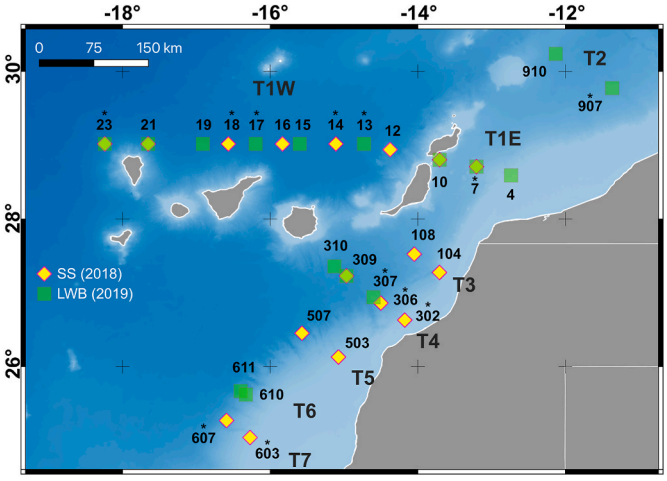

Fig. 1. Location of sampling stations: yellow diamonds stand for stations sampled during the Stratified Season (October 2018), and in green squares during the Late Winter Bloom (March 2019). Asterisks stand for night-hauls stations and number above mark-stations indicates the station number. T stands for the number of the transect.

fluorometer (FluoroWetlabECO AFLFL) calibrated using solid standard provided by the company. Temperature, salinity, oxygen, and Chl *a* sections were represented using Ocean Data View using the DIVA gridding procedure (Schlitzer, 2015). Sea surface temperature (SST) monthly average values were downloaded from the NASA Ocean Color web site for each cruise and then plotted on QGIS, and primary production was obtained for each station from the Ocean Productivity web site using the Vertical Generalized Production Model (VGPM) (Behrenfeld and Falkowski, 1997) as the standard algorithm. Stations were gathered in transects according to their location: north of the islands and west of the strait between Lanzarote and Fuerteventura was called T1W, northeast was T1E, and the rest of the stations were grouped into T2, T3, T4, T5, T6, and T7 from north to south (Fig. 1).

2.2. Image analysis

The taxonomic characterization of abundance and size distributions were performed using a representative subsample of the zooplankton community from the onboard fixed samples. In order to better represent all size classes, the subsample was divided into two categories using a 1000 μm mesh sieve and individually scanned. Thus, two images were obtained per station. Samples were imaged using an EPSON scan ver. 4990 at 2400 dpi, then processed in ZooProcess (Gorsky et al., 2010; Vandromme et al., 2012) and the resulting vignettes, along with a metadata file, were uploaded to EcoTaxa (https://ecotaxa.obs-vlfr.fr/; Picheral et al., 2017) for machine-assisted identification, using a training set developed by the authors. Both training sets were validated up to a 95% for taxonomy classification.

2.3. Zooplankton biovolume, abundance and biomass

After vignette classification, we first transformed pixel size to length and then estimated image-based equivalent spherical diameter (ESD, mm). Then, we estimated biovolume (mm^3) assuming ellipsoidal shape. Ellipsoidal volume (mm^3) was calculated as:

$$V = \frac{4\pi}{3}\left(\frac{major\ axis}{2}\right)\left(\frac{minor\ axis}{2}\right)^2$$

where major and minor axes (mm) of each object were provided by ZooProcess.

Abundances of each taxonomic zooplankton group were calculated as the number of organisms per station, and standardized to the number of organisms per cubic meter ($ind{\cdot}m^{-3}$). Biomass from the image analysis (dry mass, DM) was estimated following Maas et al. (2021), applying taxon-specific biovolume to DM conversion. Biomass was also estimated as protein content using bovine serum albumin (BSA) as the standard following the method given by Lowry et al. (1951) and modified by Rutter et al. (1968). Zooplankton protein content was converted to dry weight using the ratio of 2.49 given by Hernández-León et al. (2019) for subtropical waters, and dry weight was converted into carbon units assuming carbon content as 40% of dry weight (Dam and Peterson, 1993).

2.4. Cluster analysis

Spatial and temporal variability of zooplankton abundances were analyzed by a hierarchical clustering and similarity profile routine (SIMPROF, $p < 0.01$ and 999 permutations). The significant groups of the SIMPROF test were used as factors to test significant differences in temporal/spatial assemblages of the zooplankton using a one-way similarity analysis (ANOSIM). Data was transformed to log(x+1) to reduce the weighting of dominant species, and similar matrices were clustered using Bray-Curtis method (Clarke and Warwick, 2001). A similarity percentages (SIMPER) test was then used to determine which taxon contributed most to characterize each group (Clarke and Gorley, 2006; Clarke and Warwick, 2001). After this, and using the same Bray-Curtis similarity matrix, a non-metric multidimensional scaling (nMDS) was performed. The groups were entered into the nMDS plot to visualize the spatial ordination of the groups of samples. Moreover, the nMDS plot was represented by superimposing bubbles of increasing size related to abundance values of key taxa detected in the SIMPER analysis. These multivariate analyses were carried out using PRIMER v7.0.20.

2.5. Zooplankton normalized biomass size spectra

Detrital particles, phytoplankton, organism parts, and those smaller than 200 μm maximum axis length were removed before the normalize biomass analysis. We created size-groups (i.e. bins) according to ESD measurements, grouping data into 30 size groups of 2 mm ranging from 0.98 mm to 91.24 mm. DM from the image analysis was estimated as explained above assuming the conversion factor of a Calanoida Copepoda when the taxonomic assignment did not fall into one of the predefined categories. DM was normalized to make the spectra independent of size group by dividing the biomass of each size group by the width (i.e., lower size limit) of the size group.

The NBSS were calculated following Platt and Denman (1977): the X-axis [$\log_2$ zooplankton biomass ($mgC{\cdot}ind^{-1}$)] was calculated by dividing zooplankton biomass ($mgC{\cdot}m^{-3}$) by the abundance of each size class ($ind{\cdot}m^{-3}$) and converting to $\log_2$; the Y-axis [$\log_2$ normalized biomass ($ind{\cdot}m^{-3}$)] was calculated by dividing the biomass ($mgC{\cdot}m^{-3}$) in each size class by the interval of each size class [Δvolume (mm^3)] and converting to $\log_2$. A least-squares linear regression was fitted between the normalized biomass size spectrum (Dai et al., 2016; Quinones et al., 2003) and logarithm of the modal weight for each size group to estimate the size structure of the community from station groups obtained by clustering (Chen et al., 2020). The extreme size ranges could be subject to error resulting in curvature of the log-linear relationship at either end of the spectrum. These inflection points at the extreme size ranges of each method were not included, as they could cause potential error in the calculation of the parameters of the spectrum (Marcolin et al., 2015; San Martin et al., 2006). In addition, regressions were checked for outliers using the Bonferroni-adjusted p-value (<0.05) of studentized residuals and Cook's distance with the car package in R. When outliers were detected, regression parameters were newly estimated (Catherine et al., 2012). To identify the day-night influence within each group on the slopes of NBSS we performed an analysis of covariance (ANCOVA) using a post-hoc comparison of the slopes of fitted lines with the *lsmeans* package (Lenth and Lenth, 2018) in R. We also compared the variability between groups depending on time. In all cases, data were examined for normality using the Shapiro-Wilk test and homogeneity of variances by the Levene's test before analysis.

2.6. Data analyses

Seasonal and spatial differences in mesozooplankton biomass were tested using Kruskal-Wallis when variance homogeneity (Levene's test) or normal distribution (Shapiro-Wilk test) were not met with pairwise Wilcoxon test as post hoc test; and when the premises were not violated, an ANOVA was performed with the Tukey test as posterior test in R environment (R Core Team, 2022).

3. Results

3.1. Environmental and biotic patterns

Water column physical properties showed clear patterns at spatial and seasonal scale (Figs. 2–4) (Table 1). During the SS we observed a marked stratification across all transects dismissing as we approached the African coast (Fig. 2a,c,e; Fig. 3). By contrast, during the LWB we observed a clear mixed layer in the first 150 m depth with lower water temperature and higher Chl *a* values, particularly in the transects close

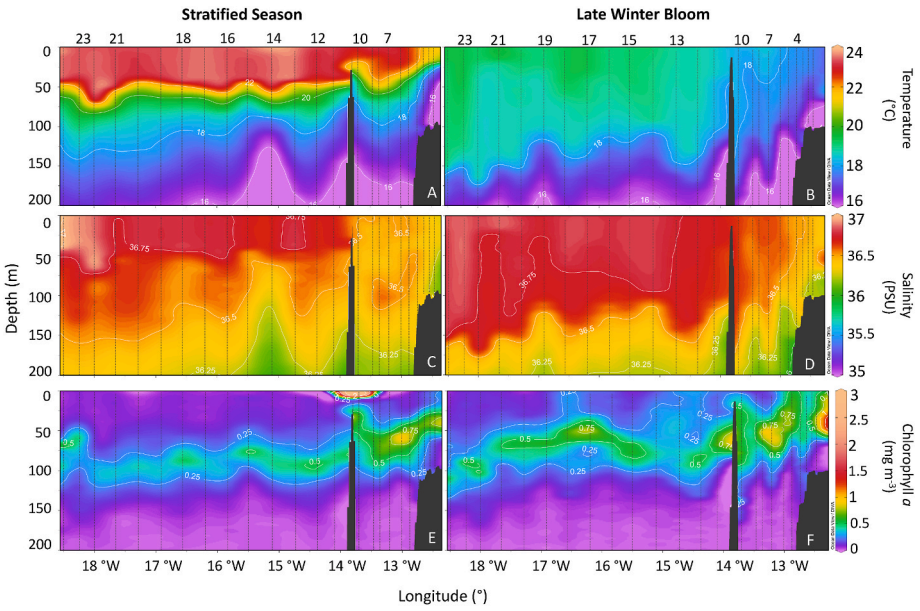

Fig. 2. Vertical sections (0–200 m) of temperature (°C) (A, B), salinity (PSU) (C, D) and chlorophyll *a* concentration (mg·m^{-3}) (E, F) during the Stratified Season (left panels) and the Late Winter Bloom (right panels) in transect T1W and T1E (see Fig. 1). Numbers on the top stand for station numbers, and black lines onside the graph for CTD-sampled stations across the transect.

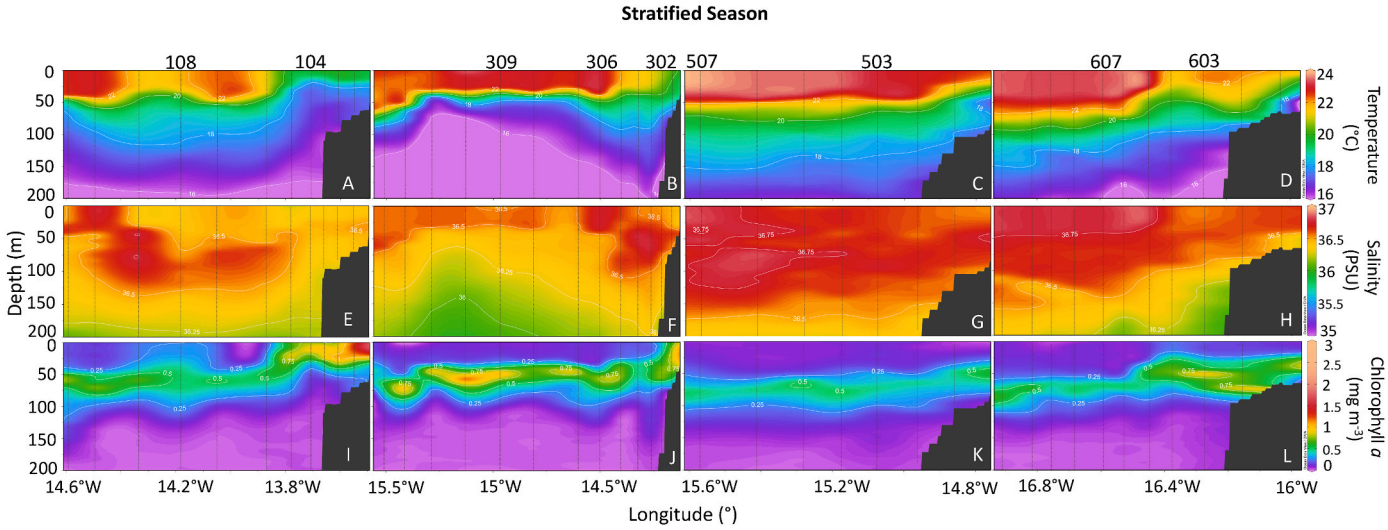

Fig. 3. Vertical section (0–200 m) of temperature (°C) (A, B, C, D), salinity (PSU) (E, F, G, H) and chlorophyll *a* concentration (mg·m^{-3}) (I, J, K, L) during the Late Winter Bloom in the stations close to the African coast (see Fig. 1). Numbers on the top stand for station numbers and black lines onside the graph for CTD-sampled stations across the transect.

to the African coast (Fig. 2b,f; Fig. 4). Average values of temperature in the upper 200 m depth were about 1 °C higher during the SS compared to the LWB. Seasonal and spatial differences in salinity were not prominent (difference of 0.1) (Table 1).

Integrated Chl *a* values were similar between both seasons, with larger differences in transect T1E. However, we found higher differences for primary production (PP) values, displaying higher values in transects inside the upwelling influenced area and showing the highest differences in oceanic water (T1) between both seasons (Table 1). The deep Chl *a* maximum was thicker and shallower during the LWB in oceanic waters (Fig. 2e and f), whereas in both cruises the signature of high Chl *a* concentration related to upwelled waters was noticeable off the African coast (Fig. 3i-l; Fig. 4g–i). Mesozooplankton biomass was higher during the LWB compared to the SS (Wilcoxon Test, $W = 574$, $p < 0.001$), reaching maximum values close to the NWA coast and decreasing towards the open ocean (Table 1). In both seasons, we generally observed higher zooplankton biomass in night-sampled stations (Fig. 5). During the LWB, zooplankton biomass was two-fold higher in T1W and 2.5-fold higher along the transects in the upwelling influenced area. However, we obtained similar values for T1E during both seasons. Comparing the upwelling influenced transects in both seasons, biomass was on average two-times higher during the LWB (Table 1). Total biomass was dominated by large organisms (>1000 μm) during the SS (Fig. 5a; ANOVA, Tukey Test, $p < 0.001$: Supplementary Material Table S1), while during the LWB medium (500–1000 μm) and small (200–500 μm) organisms contributed most to the zooplankton biomass, but only the fraction >1000 μm significantly differed from the fraction 200–500 μm (ANOVA, Tukey Test, $p < 0.05$: Supplementary Material Table S1). We found larger biomass differences during the SS between the transects close to the upwelling system. T2 presented biomass values

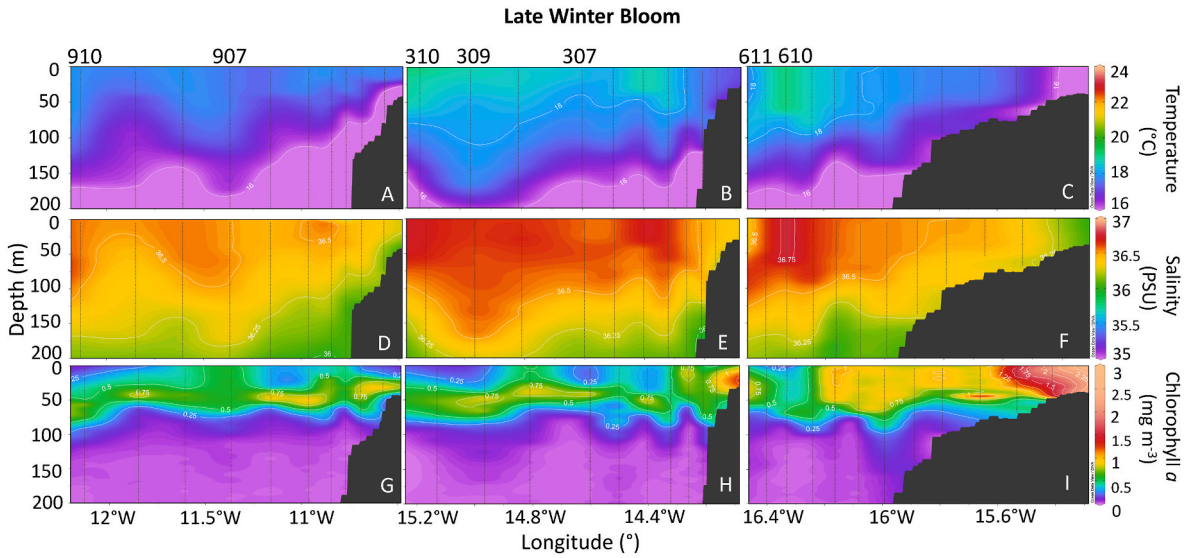

Fig. 4. Vertical section (0–200 m) of temperature (°C) (A, B, C), salinity (PSU) (D, E, F) and chlorophyll *a* concentration (mg·m^{-3}) (G, H, I) during the Stratified Season in the stations close to the African coast (see Fig. 1). Numbers on the top stand for station numbers and black lines onside the graph for CTD-sampled stations across the transect.

Table 1
Average temperature, salinity, chlorophyll *a*, primary production, and zooplankton biomass (± standard deviation) for the different transects (see text) sampled during the stratified season and the late winter bloom cruise in the upper 200 m depth. *No value available for station 10.

Season	Transect	Number of stations	Average temperature (°C)	Average salinity (PSU)	Integrated Chl *a* (mg·m^{-2})	Primary producion (mgC·m^{-2}·d^{-1})	Zooplankton biomass (mgC·m^{-2})
Stratified season	T1W	6	19.25 ± 0.54	36.54 ± 0.12	0.16 ± 0.01	325.42 ± 19.11	157.11 ± 75.77
	T1E	2	18.25 ± 0.70	36.39 ± 0.04	0.25 ± 0.02	438.99*	353.80 ± 129.48
	T3	2	17.72 ± 1.31	36.21 ± 0.19	0.20 ± 0.04	675.29 ± 282.74	85.05 ± 7.54
	T4	3	17.52 ± 0.67	36.34 ± 0.09	0.28 ± 0.12	694.82 ± 448.86	294.07 ± 17.95
	T5	2	19.70 ± 0.14	36.64 ± 0.04	0.17 ± 0.01	398.28 ± 42.34	190.03 ± 17.33
	T7	2	18.85 ± 1.10	36.48 ± 0.16	0.19 ± 0.06	379.47 ± 2.40	409.43 ± 130.54
Late Winter Bloom	T1W	6	18.20 ± 0.31	36.63 ± 0.06	0.19 ± 0.03	532.77 ± 38.32	319.77 ± 139.74
	T1E	3	17.47 ± 0.36	36.50 ± 0.08	0.32 ± 0.03	758.55 ± 123.14	386.15 ± 180.25
	T2	2	17.05 ± 0.07	36.43 ± 0.01	0.24 ± 0.01	735.79 ± 46.76	675.75 ± 250.91
	T4	3	17.57 ± 0.45	36.51 ± 0.07	0.20 ± 0.05	796.06 ± 48.32	526.75 ± 114.14
	T6	2	17.51 ± 0.03	36.49 ± 0.01	0.18 ± 0.02	900.33 ± 78.37	691.39 ± 168.10

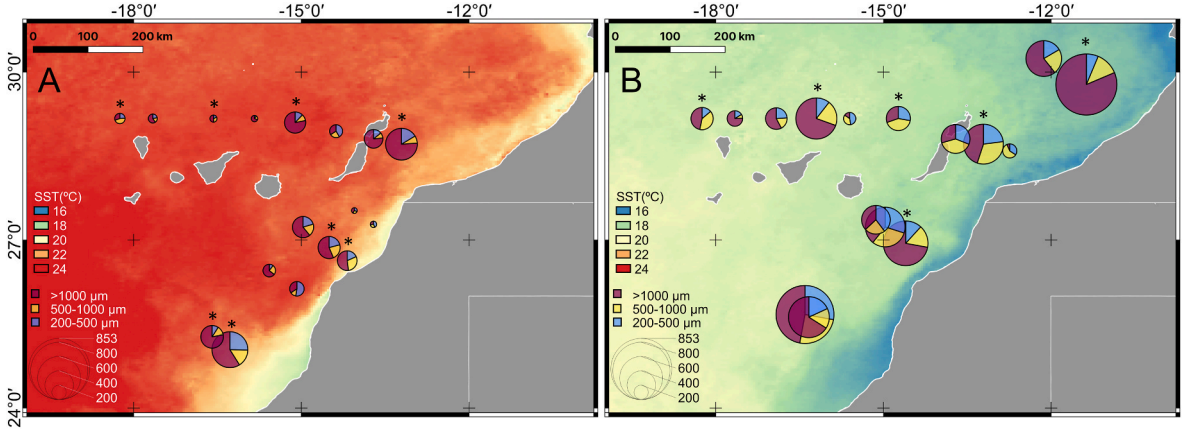

Fig. 5. Spatial distribution of the percentages of zooplankton size-fractionated biomass obtained as protein content during the Stratified Season (A) and the Late Winter Bloom (B). Bubble size represent total biomass (mgC·m^{-2}). Colors on the maps correspond to monthly-mean sea surface temperature during October (2018) for the Stratified Season and March (2019) for the Late Winter Bloom. Asterisks stand for night-hauls stations.

2-fold lower than the other transects, with a higher contribution of medium and small-size organisms in contrast to the other stations where 70% of the biomass was due to large-size organisms.

3.2. Zooplankton structure

The SIMPROF test differentiated three main groups of stations ($p <$

0.001) with a similarity of 80%: (1) the Upwelling-group composed by stations from the upwelling zone regardless of the season, (2) the LWB-group, and (3) the SS-group, with stations sampled according to the season. The station 603 sampled during the SS was not clustered in any of the three groups of stations. The ANOSIM tests (R-statistic = 0.779, p < 0.001) also confirmed the significance of these gatherings (Fig. 6a), as well as the nMDS ordination (Fig. 6b). The SIMPER analysis showed the contribution of each taxonomic group (%) to the dissimilarity between the three groups (Upwelling, LWB, and SS, Table 2; Fig. 6c and d). Calanoida Copepoda were the taxon most contributing to the similarity in each group due to their high abundance, but they did not contribute to distinguish the SIMPROF groups. *Penilia* spp. and *Evadne* spp. accounted for the 27% of the dissimilarity to differentiate the Upwelling-group from the SS-group, whereas Salpidae and Appendicularia together contributed with the 14.5% of dissimilarity (Table 2). Cladocera and Appendicularia were also key taxa to discriminate the Upwelling-group from the LWB-group (almost 17% and 8.5% of dissimilarity, respectively), and Euphausiacea became important and accounting for almost 6% of the dissimilarity. Finally, the differences between the LWB- and SS-groups, were mostly driven by the Salpidae (13.9% of dissimilarity), followed by eggs (8.2%), Pteropoda and Heteropoda (6.7%), and other gastropod molluscs (6.5%).

3.3. Normalized biomass size distribution characterization

Overall NBSS slopes of mesozooplankton size spectra were fitted with a linear relationship, ranging from −0.45 to −1.73 (Fig. 7, Table 3). The elevations were remarkably constant in the SS-group (6.22 for day, and 6.48 for night), and variable in the LWB-group, ranging from 6.03 (day) to 7.06 (night). The Upwelling-group showed the lowest regression coefficient ($r^2 < 0.62$), with high errors in the estimation of linear parameters, a non-homogeneous distribution, and low number of samples (Fig. 7c; Table 3). Given that these biases can lead to misinterpretation of the ANCOVA analysis, we decided to not include it as a preventive measure. The overall NBSS slope for the SS-group on day (−0.97) was significantly different from those at night (−0.80; ANCOVA, F = 4.52, p = 0.036; Fig. 7a), indicating a higher proportion of large-sized zooplankton during the night, mainly Euphausiacea. While Chaetognatha were the main daytime organisms during the SS, Euphausiacea dominated the community at night (Fig. 8c and d). Although any diel variation was observed between the slopes for the LWB-group (ANCOVA, F = 0.02, p = 0.89), the large value of the intercept at night (7.056 ± 0.208) in relation to daytime (6.03 ± 0.22) also showed a clear effect of DVM in the NBSS. The difference with the SS was the increased zooplankton biomass of smaller size fractions at night. This group was characterized by the large presence of Hydrozoa and Salpidae during the day and the night, with less Euphausiacea during the night compared to the SS-group. Comparing groups, the SS-group was characterized by a steeper NBSS slope (−0.969) than the LWB-group (−0.753; ANCOVA, F = 6.283, p = 0.014; Fig. 7b) for daytime, but both groups showed similar values (−0.802 and −0.743, respectively) during nighttime (ANCOVA, F = 0.763, p = 0.385). Biomass in each size bin (Fig. 8) showed similar taxa distribution for the smaller size bins, with high abundance of Copepoda such as Calanoida, *Oncaea* spp., and *Corycaeus* spp., Appendicularia, and Salpidae. As the bin increased, the taxa distribution shifted towards a community mainly dominated by Salpidae and Hydrozoa in the LWB-group, and by Chaetognatha and Euphausiacea in the SS-group.

4. Discussion

4.1. Spatial and temporal patterns in the C-ATZ

Mesozooplankton biomass, abundance, and size distribution were

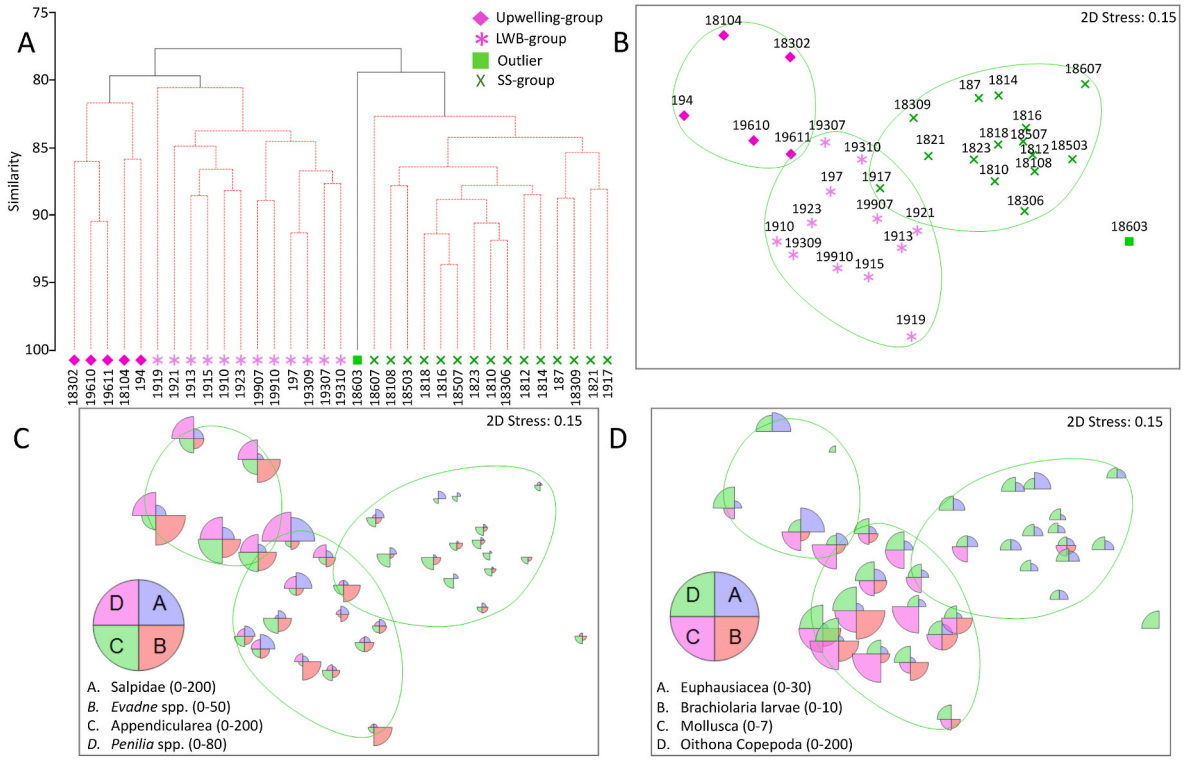

Fig. 6. A) Assemblages of zooplankton structure according to the abundance and composition for each sampled season and area. First two numbers of the x-labels correspond to the sampling year, and the rest to the code of the station as in Fig. 1. B) Results of the non-metric multidimensional scaling (nMDS) of zooplankton communities. C and D) Zooplankton taxonomic composition of the key organisms. Pink diamonds stand for those stations performed close to the upwelling African coast, pink asterisks stand for those stations sampled during the Late Winter Bloom, green squares correspond to an outgroup, and green crosses to stations performed during the Stratified season. Bubble size stand for abundance values for each selected taxon (number·m^{-3}).

Table 2
Taxa regarded as discriminators between the zooplankton community assemblages from the SIMPER analysis up to a 70%.

	Upwelling-group vs SS-group		Upwelling-group vs LWB-group		LWB-group vs SS-group	
	Dissimilarity (%)	Contribution (%)	Dissimilarity (%)	Contribution (%)	Dissimilarity (%)	Contribution (%)
Penilia sp.	4.05	16.13	2.11	10.38	1.41	5.46
Evadne sp.	2.71	10.82	1.34	6.58	1.54	5.94
Salpidea	1.88	7.5	0.95	4.68	3.61	13.9
Appendicularia	1.75	6.99	1.73	8.52		
Corycaeidae copepoda	1.25	4.97	0.82	4.01		
Euphausiacea	1.17	4.67	1.22	5.98	1.28	4.94
Other Gastropoda	1.11	4.43			1.68	6.48
Echinodermata-larvae	1.03	4.11	0.92	4.53		
Polychaeta	1	3.98	0.76	3.74		
Egg	0.97	3.88	0.75	3.7	2.14	8.22
Pteropoda + Heteropoda	0.85	3.39	0.93	4.58	1.75	6.74
Brachiolaria			0.96	4.74	1.42	5.46
Oithona copepoda			0.95	4.67		
Siphonophorae			0.86	4.24		
Ostracoda					1.3	4.99
Foraminifera					1.15	4.43
Chaetognatha					1.02	3.91

spatially and temporarily determined in the C-ATZ. We detected clear environmental and community differences between the SS and LWB seasons, similar to those already reported before for this area (Braun, 1979; Hernández-León, 1988; Hernández-León et al., 2007; Valdés and Déniz-González, 2015). We found a quite stratified water column with a sharp thermocline between 50 and 70 m depth, low integrated Chl *a,* and PP values during the SS, especially north of the Canary Islands. By contrast, water column properties during the LWB showed a wide mixed layer, and higher integrated Chl *a,* and PP values, as well as a shallower distribution of the deep Chl *a* maximum. Previous works in the C-ATZ studied the influence of the spatial and annual variability of the water column, mesoscale activity, and the upwelling and its filaments on plankton (see Hernández-León et al., 2007). We detected higher zooplankton biomass during the LWB enhanced by higher PP values, particularly noteworthy in the upwelling influenced area since the water intrusion pulses close to shore create large phytoplankton biomass events (Reyes-Mendoza et al., 2019). A relative high zooplankton biomass barely varied around the area between both the Cape Ghir and Cape Juby (T1E) due to a quasi-permanent upwelling filament off Cape Ghir and the intermittent filament off Cape Juby (Berraho et al., 2015). Finally, size fractionated mesozooplankton biomass showed a higher biomass of the larger size groups during the SS, as they have longer generation times than primary producers and therefore survive for longer periods. Also, a succession of small to medium and large Calanoida and gelatinous organisms from the upwelled waters to the ocean is normally the rule (Postel, 1990). These results suggest that the oceanographic conditions drive the mesozooplankton biomass, with clear environmental and ecological differences during the annual cycle in the studied area.

4.2. Abundance and composition

Despite the wide variability of mesozooplankton biomass from the upwelling influenced area to offshore through the annual cycle, the common feature throughout the C-ATZ is the numerical dominance of Copepoda determined by the seasonality and the upwelling regime. Beside Copepoda, the organisms characterizing each season were Hydrozoa and Salpidae during the LWB, and Chaetognata and Euphausiacea during the SS. However, these organisms were not the key to cluster the stations into the three main groups. The difference between station groups was characterized by the abundance of seasonal organisms such as *Evadne* spp. and *Penilia* spp., as similarly reported by Hernández-León et al. (2007). Several studies in the area have demonstrated that Cladocera dominate along filaments of upwelled waters, as well as fish larvae (Hernández-León et al., 2007; Moyano et al., 2009). Cladocera burst in eutrophic areas (Liu et al., 2014), and constitute the main prey for fish, therefore their populations are affected by phytoplankton production and fish predation (Gliwicz et al., 2004). Moreover, the abundance of Salpidae helped to distinguish the intergroups variability. These organisms have a high grazing impact that can deplete the photic zone of phytoplankton and export huge quantities of organic matter to the deep sea (Dadon-Pilosof et al., 2019). Abundance might be used as an indicator of shifts in the community due to changes in the environmental conditions (e.g. temperature, chlorophyll, or water column stability) (Coyle et al., 2008). For instance, Copepoda differed between coastal and offshore waters, denoting a more structured assemblage with higher species diversity and evenness offshore (Berraho et al., 2015), with different species throughout the annual cycle (Corral, 1970). Moreover, weak upwelling conditions or even a strong seasonality in the Canary Current System entail low levels of productivity during the cold season close to North of Cape Beddouza (35°48′N). It affects the zooplankton with low abundances and a high dominance of Copepoda. However, the zooplankton is less structured and balanced during the upwelling season (in summer), predominating few species but with high abundances (Berraho et al., 2015). The increase of water temperature and the decrease in food along the offshore have been considered as the main factors influencing the zooplankton body size, thus the NBSS slope, because of the size-dependent energy requirements needed to maintain basal metabolism (Brown et al., 2004; Ikeda, 1985; Zhou, 2006). Consequently, a size gradient from small to medium and large Calanoida and gelatinous organisms, such as Thaliacea and Siphonophorae, from the upwelled waters to the ocean is normally the rule (Postel, 1990) as observed here for the NBSS slopes. Nevertheless, this is the first report on the zooplankton assemblages in the C-ACTZ and the general patterns need to be corroborated and complemented with additional studies at local and regional scales.

4.3. Normalized biomass size spectra

Size spectra obtained in this study showed a strong seasonal change in the zooplankton size structure and production off the C-ATZ in response to hydrological conditions, and a spatial separation between the upwelling area and the Canary Islands. Size-based normalized biomass/biovolume size spectra have been considered a tool of interest for plankton energy fluxes and the evaluation of the marine ecosystems structure (Dai et al., 2016; Platt and Denman, 1977; Quinones et al., 2003; Suthers et al., 2006). However, the way in which size diversity impacts the functioning of the ecosystem is an important but unclear question. The theory suggests that the NBSS slope in a stable marine ecosystems should be settled at approximately −1 (Sprules and

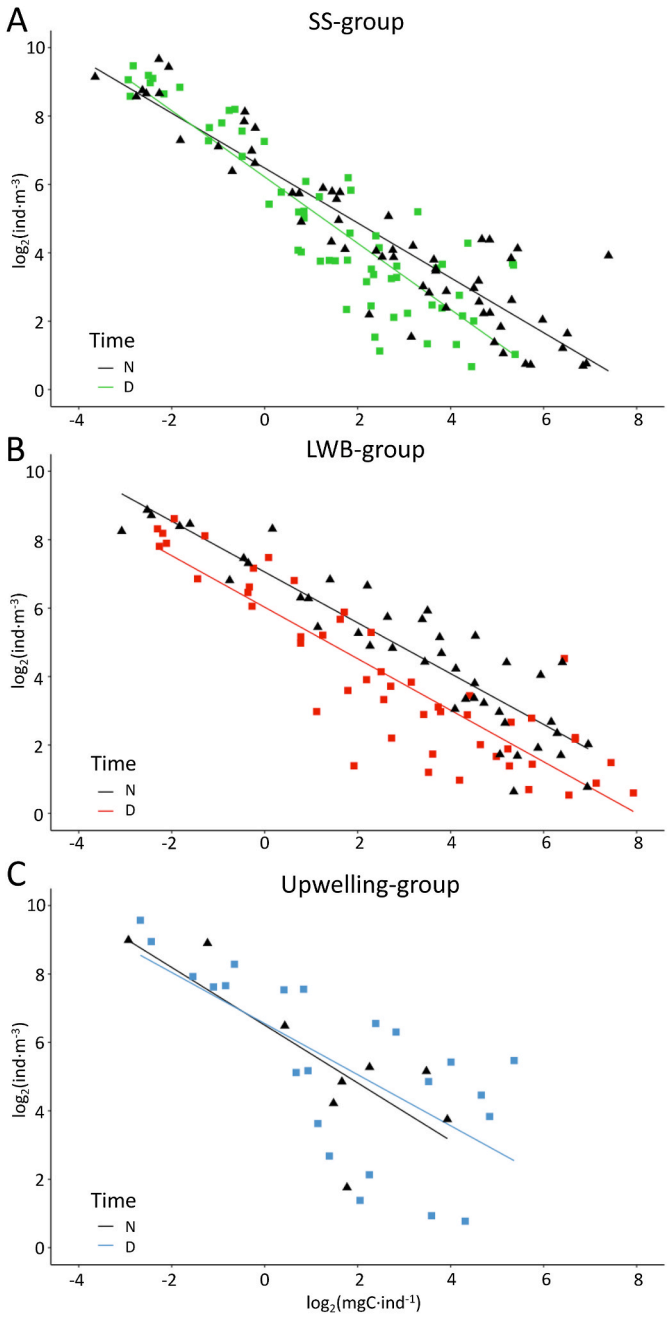

Fig. 7. Mesozooplankton NBSS for the grouped stations according to Fig. 6a cluster: A) SS-group, B) LWB-group, and C) Upwelling-group. Color in each NBSS corresponds to day hauls, and black for night hauls.

Munawar, 1986). Even so, theoretical models and empirical studies still have some discrepancies, especially in strongly dynamic ecosystems where energy pulses through the system might unbalance the theoretical linearity of the system (Quinones et al., 2003; Sourisseau and Carlotti, 2006). Steeper slopes are generally related to a biomass decline with increasing size, thus lower transfer efficiency for higher trophic levels, to an increase of predation pressure on the smallest zooplankton (Brown et al., 2004; Noyon et al., 2022; San Martin et al., 2006; Zhou, 2006), and to higher abundance of herbivorous zooplankton organisms, usually smaller in size compared to carnivorous species (Noyon et al., 2022). Moreover, some studies argued that this pattern could also occur due to the increase of juvenile organisms linked to an enhanced reproduction stimulated by food availability (García-Comas et al., 2014; Giering et al., 2019), whereas others authors link steeper slopes to oligotrophic and warmer waters where the conditions are more stable (Canales et al., 2016; Medellín-Mora et al., 2020; Sprules and Munawar, 1986). Our results showed steeper slopes for the SS-group, in agreement with oligotrophy conditions, higher water temperatures and water column stratification, previously reported by Hernández-León et al. (2007) and also obtained in this study. This outcome suggests an overall increase in predation pressure with size, and a loss of available energy to higher trophic levels during that season, thus a strong bottom-up control during the SS linked to food-limitation conditions.

On the other hand, the LWB-group showed more gradual slopes, with the highest intercepts, suggesting a wider size biomass distribution. During this season, the thermocline is eroded allowing nutrients to reach the euphotic zone enhancing primary and mesozooplankton production (Schmoker et al., 2012). The high productivity and lower water temperatures favored the abundance of different size spectra organisms flattening the LWB slopes and promoting higher trophic efficiency. This result was also obtained by García-Comas et al. (2014), showing also that food (Chl *a* concentration) overrides the influence of water temperature, being the trophic status the main factor influencing zooplankton size structure. In this sense, our results followed the theoretical models increasing the relative abundance of large organisms with increased energy availability. Schmoker and Hernández-León (2013) found that in the subtropical waters of the Canary Islands, microplankton are actively grazing on picoplankton and on heterotrophic prokaryotes, and they are being, in turn, grazed by small mesozooplankton, highlighting the most likely top-down control of higher trophic levels on lower trophic levels existing in the planktonic food web. Moreover, increasing zooplankton size and taxonomic diversity enhances top-down control on phytoplankton (Ye et al., 2013). Thus, it seems that during the LWB the food webs are controlled by top-down processes.

Theoretically, less stable environments have higher secondary structuring processes and disturbances around the linear NBSS slope, lowering the r^2 value (De Souza et al., 2020; Sprules and Barth, 2016). Low r^2 values denote that the community is unstructured or in a non-equilibrium state (Boudreau et al., 1991; Thiebaux and Dickie, 2011), while values close to 1 indicate communities close to steady-state equilibrium. The SS-group and the LWB-group showed similar r^2 values, ranging from 0.79 to 0.84 from day to night hauls, respectively

Table 3
Results from the linear regressions of the Normalized Biomass Size Spectra analysis. n: number of data points.

Cluster	Period	Intercept		Slope		R^2	n	Number of stations
		Range	Mean ± SD	Range	Mean ± SD			
SS-group	Night	5.47 to 7.29	6.48 ± 0.17	−0.70 to −1.12	−0.80 ± 0.05	0.84	61	7
	Day	5.49 to 7.12	6.22 ± 0.18	−0.84 to −1.45	−0.97 ± 0.07	0.79	61	8
LWB-group	Night	6.62 to 7.93	7.06 ± 0.21	−0.61 to −0.95	−0.74 ± 0.05	0.84	44	5
	Day	5.38 to 7.16	6.03 ± 0.22	−0.73 to −1.67	−0.75 ± 0.06	0.79	51	7
UP-group	Night	6.50	6.50 ± 0.60	−0.84	−0.84 ± 0.25	0.62	9	1
	Day	5.74 to 7.53	6.55 ± 0.49	−0.49 to −1.73	−0.75 ± 0.18	0.47	23	4

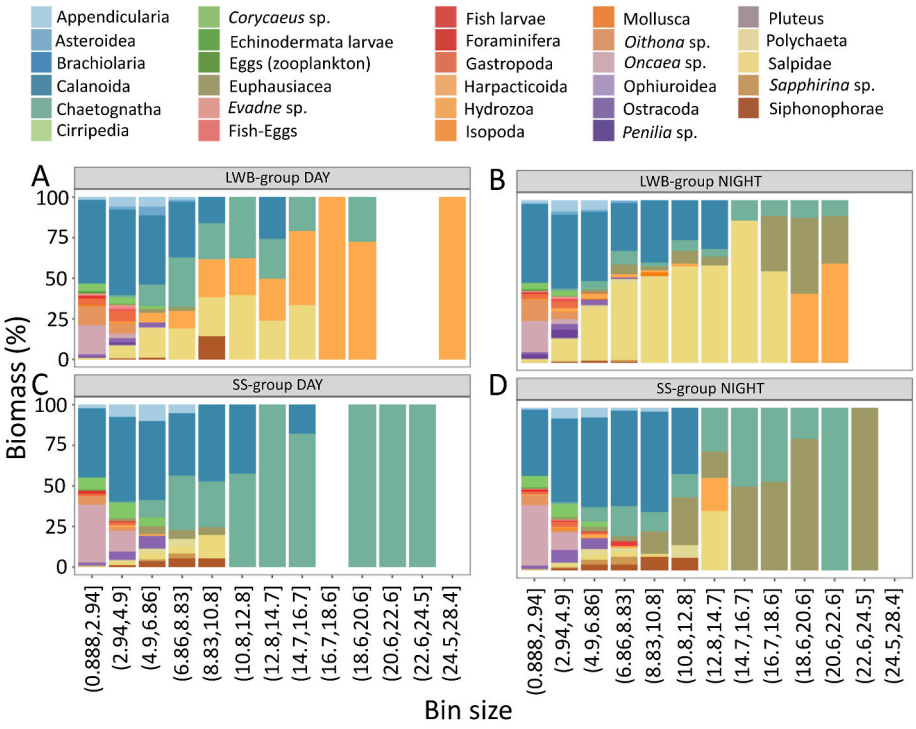

Fig. 8. Mesozooplankton biomass (%) in each bin size for the different grouped stations according to Fig. 6a cluster. A) Correspond to the LWB-group during day, B) to the LWB-group during night, C) to the SS-group during day, and D) to the SS-group during night. The Upwelling group was not included in the graph (see text).

(Table 3). This finding suggest a higher structured community than in the UP-group. In the latter group, size diversity instead of size spectrum could be a better approach for species diversity analysis and the understanding of an upwelling area. This parameter measures the continuous distribution of body size as the size deviation, which may represent an important functional diversity metric when determining the structure and functioning of a highly unstable aquatic ecosystem. Higher size diversity has higher efficiency of resource use; therefore, higher size diversity of zooplankton can increase zooplankton biomass, and the effect on trophic structure may have important management implications in aquatic ecosystems (Sun et al., 2021; Ye et al., 2013). The UP-group stations were characterized by the area they were sampled, not by the season, suggesting that zooplankton there display different properties than in oligotrophic areas. Patterns of zooplankton in the C-ATZ are scarce (see Hernández-León et al., 2007), and the taxonomic composition and distribution from the coast to the open ocean during the annual cycle remains still unknown.

Changes in zooplankton community size structure have the potential to alter the food web structure, thus the food quantity and quality for planktivorous fish (Lomartire et al., 2021; Pitois et al., 2021). In this sense, the SS-group showed the strongest day-nighttime variability in the size structure spectra, meaning a strong shift of the community in a daily period. This phenomenon is commonly attributed to diel vertical migrations (DVM) where intermediate-sized specimens perform the largest DVM (Manríquez et al., 2012; Ohman and Romagnan, 2016; Rodriguez and Mullin, 1986). Consequences of changes in the size structure due to DVM are diverse indicating the state of the food web (Brierley, 2014). The C-ATZ is part of a wider system with different physical and biological features that provide large amounts of carbon that eventually is converted into fish biomass, supporting local pelagic fisheries. Therefore, planktonic size structure (Barnes et al., 2011; Woodworth-Jefcoats et al., 2013) need to be considered for the management and assessment of fishing resources addressing the size-dependent prey-predator relationships (Canales et al., 2016), and routinely monitoring.

5. Conclusions

In conclusion, our abundance results show the differences between the upwelling area and the transitional-open ocean area, while the size spectra show the shift in the control of the food webs trophic structure throughout the annual cycle. Our finding highlights the importance of taxonomic and size spectra studies in the C-ATZ for the evaluation of the ecosystem structure and prey-predator interaction with higher trophic levels.

Author statement

MC contributed to the sampling onboard, laboratory analysis, and data processing. JML contributed to the abundance analyses. VMT contributed to the size spectra analysis. AS-L contributed to the data analysis and laboratory experiments. PV-B acted as the cruise leader. SHL supervised this study and contributed to the editing of the manuscript. All authors contributed to article writing and discussion, approving the submitted version.

Declaration of competing interest

The authors declare that they have no known competing financial interests or personal relationships that could have appeared to influence the work reported in this paper.

Data availability

Data will be made available on request.

Acknowledgments

The authors would like to thank Emilio Marañón for his useful comments on the manuscript. This study was partially funded by the Spanish Ministry project DESAFÍO (PID 2020- 118118RB-100), TRIATLAS (Grant Agreement 817578), and SUMMER (Grant Agreement

817806). María Couret was supported by a postgraduate grant (TESIS2022010116) from the Agencia Canaria de Investigación, Innovación y Sociedad de la Información (ACIISI). Airam Sarmiento-Lezcano was supported by a postgraduate grant from the Spanish Ministry of Science and Innovation (BES-2017-082540). José Landeira was supported by the Beatriz Galindo individual grant BEAGAL 18/00172.

Appendix A. Supplementary data

Supplementary data to this article can be found online at https://doi.org/10.1016/j.marenvres.2023.105976.

References

Arístegui, J., Barton, E.D., Tett, P., Montero, M.F., García-Muñoz, M., Basterretxea, G., Cussatlegras, A.S., Ojeda, A., De Armas, D., 2004. Variability in plankton community structure, metabolism, and vertical carbon fluxes along an upwelling filament (Cape Juby, NW Africa). Prog. Oceanogr. 62, 95–113. https://doi.org/10.1016/j.pocean.2004.07.004.

Armengol, L., Calbet, A., Franchy, G., Rodríguez-Santos, A., Hernández-León, S., 2019. Planktonic food web structure and trophic transfer efficiency along a productivity gradient in the tropical and subtropical Atlantic Ocean. Sci. Rep. 9, 1–19. https://doi.org/10.1038/s41598-019-38507-9.

Atkinson, A., Lilley, M.K.S., Hirst, A.G., McEvoy, A.J., Tarran, G.A., Widdicombe, C., Fileman, E.S., Woodward, E.M.S., Schmidt, K., Smyth, T.J., Somerfield, P.J., 2021. Increasing nutrient stress reduces the efficiency of energy transfer through planktonic size spectra. Limnol. Oceanogr. 66, 422–437. https://doi.org/10.1002/LNO.11613.

Barnes, C., Irigoien, X., De Oliveira, J.A.A., Maxwell, D., Jennings, S., 2011. Predicting marine phytoplankton community size structure from empirical relationships with remotely sensed variables. J. Plankton Res. 33, 13–24. https://doi.org/10.1093/PLANKT/FBQ088.

Barton, E.D., Aristegui, J., Tett, P., Canton, M., García-Braun, J., Hernández-León, S., Nykjaer, L., Almeida, C., Almunia, J., Ballesteros, S., Basterretxea, G., Escanez, J., García-Weill, L., Hernández-Guerra, A., López-Laatzen, F., Molina, R., Montero, M. F., Navarro-Peréz, E., Rodríguez, J.M., Van Lenning, K., Vélez, H., Wild, K., 1998. The transition zone of the Canary Current upwelling region. Prog. Oceanogr. 41, 455–504. https://doi.org/10.1016/S0079-6611(98)00023-8.

Batchelder, H.P., Daly, K.L., Davis, C.S., Ji, R., Ohman, M.D., Peterson, W.T., Runge, J.A., 2013. Climate impacts on zooplankton population dynamics in coastal marine ecosystems. Oceanography 26, 34–51.

Behrenfeld, M.J., Falkowski, P.G., 1997. Photosynthetic rates derived from satellite-based chlorophyll concentration. Limnol. Oceanogr. 42, 1–20. https://doi.org/10.4319/lo.1997.42.1.0001.

Berraho, A., Somoue, L., Hernández-León, S., Valdés, L., 2015. Zooplankton in the canary current large marine ecosystem. IOC-UNESCO. In: Vald, L., Déniz-González, I. (Eds.), Oceanographic and Biological Features in the Canary Current Large Marine Ecosystem. IOC Tech. Ser. No. 115, Paris, pp. 183–195. URI.

Bertram, D.F., Mackas, D.L., McKinnell, S.M., 2001. The seasonal cycle revisited: interannual variation and ecosystem consequences. Prog. Oceanogr. 49, 283–307. https://doi.org/10.1016/S0079-6611(01)00027-1.

Boucher, J., 1982. Peuplement de copépodes des upwellings côtiers nord-ouest africains: I. Composition faunistique et structure démographique. Oceanol. Acta 4, 49–62.

Boudreau, P.R., Dickie, L.M., Kerr, S.R., 1991. Body-size spectra of production and biomass as system-level indicators of ecological dynamics. J. Theor. Biol. 152, 329–339. https://doi.org/10.1016/S0022-5193(05)80198-5.

Braun, J.G., 1979. Estudios de producción en aguas de las Islas Canarias. 1. Hidrografía, nutrientes y producción primaria. Boletín Inst. Español Oceanogr. 285, 140–154.

Braun, L.M., Brucet, S., Mehner, T., 2021. Top-down and bottom-up effects on zooplankton size distribution in a deep stratified lake. Aquat. Ecol. 55, 527–543. https://doi.org/10.1007/s10452-021-09843-8.

Brierley, A.S., 2014. Diel vertical migration. Curr. Biol. 24, R1074–R1076. https://doi.org/10.1016/j.cub.2014.08.054.

Brown, J.H., Gillooly, J.F., Allen, A.P., Savage, V.M., West, G.B., 2004. Toward a metabolic theory of ecology. Ecology 85, 1771–1789.

Buitenhuis, E.T., Rivkin, R.B., Séailley, S., Le Quéré, C., 2010. Biogeochemical fluxes through microzooplankton. Global Biogeochem. Cycles 24. https://doi.org/10.1029/2009GB003601.

Canales, M.T., Law, R., Blanchard, J.L., 2016. Shifts in plankton size spectra modulate growth and coexistence of anchovy and sardine in upwelling systems. Can. J. Fish. Aquat. Sci. 73, 611–621. https://doi.org/10.1139/CJFAS-2015-0181/ASSET/IMAGES/CJFAS-2015-0181IEQ22.GIF.

Carpenter, S.R., Kitchell, J.F., Hodgson, J.R., Cochran, P.A., Elser, J.J., Elser, M.M., Lodge, D.M., Kretchmer, D., He, X., von Ende, C.N., 1987. Regulation of lake primary productivity by food web structure. Ecology 68, 1863–1876.

Catherine, A., Escoffier, N., Belhocine, A., Nasri, A.B., Hamlaoui, S., Yéprémian, C., Bernard, C., Troussellier, M., 2012. On the use of the FluoroProbe®, a phytoplankton quantification method based on fluorescence excitation spectra for large-scale surveys of lakes and reservoirs. Water Res. 46, 1771–1784. https://doi.org/10.1016/J.WATRES.2011.12.056.

Chen, Y., Lin, S., Wang, C., Yang, J., Sun, D., 2020. Response of size and trophic structure of zooplankton community to marine environmental conditions in the northern South China Sea in winter. J. Plankton Res. 42, 378–393. https://doi.org/10.1093/PLANKT/FBAA022.

Cianca, A., Helmke, P., Mouriño, B., Rueda, M.J., Llinás, O., Neuer, S., 2007. Decadal analysis of hydrography and in situ nutrient budgets in the western and eastern North Atlantic subtropical gyre. J. Geophys. Res. Ocean. 112, 7025. https://doi.org/10.1029/2006JC003788.

Clarke, K.R., Gorley, R.N., 2006. PRIMER V6: User Manual/Tutorial. Prim, Plymouth, p. 192.

Clarke, K.R., Warwick, R.M., 2001. Change in marine communities. An approach to Stat. Anal. Interpret. 2, 1–68.

Corral, J., 1970. Contribución al conocimiento del plancton de Canarias. Tesis Dr. Univ, Madrid, p. 343.

Cottingham, K.L., 1999. Nutrients and zooplankton as multiple stressors of phytoplankton communities: evidence from size structure. Limnol. Oceanogr. 44, 810–827.

Coyle, K.O., Pinchuk, A.I., Eisner, L.B., Napp, J.M., 2008. Zooplankton species composition, abundance and biomass on the eastern Bering Sea shelf during summer: the potential role of water-column stability and nutrients in structuring the zooplankton community. Deep Sea Res. Part II Top. Stud. Oceanogr. 55, 1775–1791. https://doi.org/10.1016/J.DSR2.2008.04.029.

Cózar, A., García, C.M., Gálvez, J.A., 2003. Analysis of plankton size spectra irregularities in two subtropical shallow lakes (Esteros del Iberá, Argentina). Can. J. Fish. Aquat. Sci. 60, 411–420. https://doi.org/10.1139/F03-037.

Dadon-Pilosof, A., Lombard, F., Genin, A., Sutherland, K.R., Yahel, G., 2019. Prey taxonomy rather than size determines salp diets. Limnol. Oceanogr. 64, 1996–2010.

Dai, L., Li, C., Tao, Z., Yang, G., Wang, X., Zhu, M., 2017. Zooplankton abundance, biovolume and size spectra down to 3000 m depth in the western tropical North Pacific during autumn 2014. Deep-Sea Res. Part I Oceanogr. Res. Pap. 121, 1–13. https://doi.org/10.1016/J.DSR.2016.12.015.

Dai, L., Li, C., Yang, G., Sun, X., 2016. Zooplankton abundance, biovolume and size spectra at western boundary currents in the subtropical North Pacific during winter 2012. J. Mar. Syst. 155, 73–83.

Dai, Luping, Li, C., Yang, G., Sun, X., 2016. Zooplankton abundance, biovolume and size spectra at western boundary currents in the subtropical North Pacific during winter 2012. J. Mar. Syst. 155, 73–83. https://doi.org/10.1016/J.JMARSYS.2015.11.004.

Dam, H.G., Peterson, W.T., 1993. Seasonal contrasts in the diel vertical distribution, feeding behavior, and grazing impact of the copepod Temora longicornis in Long Island Sound. J. Mar. Res. 51, 561–594. https://doi.org/10.1357/0022240933223972.

De Souza, C.S., Da Conceicão, L.R., Freitas, T.S.S., Aboim, I.L., Schwamborn, R., Neumann-Leitão, S., Mafalda Junior, P.D.O., 2020. Size spectra modeling of mesozooplankton over a tropical continental shelf. J. Coast Res. 36, 795–804. https://doi.org/10.2112/JCOASTRES-D-19-00102.1.

García-Comas, C., Chang, C.Y., Ye, L., Sastri, A.R., Lee, Y.C., Gong, G.C., Hsieh, C. hao, 2014. Mesozooplankton size structure in response to environmental conditions in the East China Sea: how much does size spectra theory fit empirical data of a dynamic coastal area? Prog. Oceanogr. 121, 141–157. https://doi.org/10.1016/J.POCEAN.2013.10.010.

Giering, S.L.C., Wells, S.R., Mayers, K.M.J., Schuster, H., Cornwell, L., Fileman, E.S., Atkinson, A., Cook, K.B., Preece, C., Mayor, D.J., 2019. Seasonal variation of zooplankton community structure and trophic position in the Celtic Sea: a stable isotope and biovolume spectrum approach. Prog. Oceanogr. 177, 101943 https://doi.org/10.1016/J.POCEAN.2018.03.012.

Gliwicz, M.Z., Jawiński, A., Pawłowicz, M., 2004. Cladoceran densities, day-to-day variability in food selection by smelt, and the birth-rate-compensation hypothesis. Hydrobiologia 526, 171–186. https://doi.org/10.1023/B:HYDR.0000041605.72338.22.

Gómez-Gesteira, M., De Castro, M., Álvarez, I., Lorenzo, M.N., Gesteira, J.L.G., Crespo, A. J.C., 2008. Spatio-temporal upwelling trends along the canary upwelling system (1967–2006). Ann. N. Y. Acad. Sci. 1146, 320–337. https://doi.org/10.1196/ANNALS.1446.004.

Gorsky, G., Ohman, M.D., Picheral, M., Gasparini, S., Stemmann, L., Romagnan, J.B., Cawood, A., Pesant, S., García-Comas, C., Prejger, F., 2010. Digital zooplankton image analysis using the ZooScan integrated system. J. Plankton Res. 32, 285–303. https://doi.org/10.1093/PLANKT/FBP124.

Hays, G.C., Richardson, A.J., Robinson, C., 2005. Climate change and marine plankton. Trends Ecol. Evol. 20, 337–344. https://doi.org/10.1016/j.tree.2005.03.004.

Heath, M.R., 1995. Size spectrum dynamics and the planktonic ecosystem of Loch Linnhe. ICES J. Mar. Sci. 52, 627–642. https://doi.org/10.1016/1054-3139(95)80077-8.

Hernández-León, S., 1988. Ciclo anual de la biomasa del mesozooplancton sobre un área de plataforma en aguas del Archipiélago Canario. Investig. Pesq. [ISSN 0020-9953] 52 (1), 3–16.

Hernández-León, S., Almeida, C., Portillo-Hahnefeld, A., Gómez, M., Rodríguez, J.M., Arístegui, J., 2002b. Zooplankton biomass and indices of feeding and metabolism in relation to an upwelling filament off northwest Africa. J. Mar. Res. 60, 327–346. https://doi.org/10.1357/00222400260497516.

Hernández-León, S., Calles, S., Fernández de Puelles, M.L., 2019. The estimation of metabolism in the mesopelagic zone: disentangling deep-sea zooplankton respiration. Prog. Oceanogr. 178, 102163 https://doi.org/10.1016/j.pocean.2019.102163.

Hernández-León, S., Gómez, M., Arístegui, J., 2007. Mesozooplankton in the canary current system: the coastal-ocean transition zone. Prog. Oceanogr. 74, 397–421. https://doi.org/10.1016/j.pocean.2007.04.010.

Hernández-León, S., Gómez, M., Pagazaurtundua, M., Portillo-Hahnefeld, A., Montero, I., Almeida, C., 2002a. Vertical distribution of zooplankton in Canary Island waters:

implications for export flux. Deep. Res. Part I Oceanogr. Res. Pap. 48, 1071–1092. https://doi.org/10.1016/S0967-0637(00)00074-1.
Hooff, R.C., Peterson, W.T., 2006. Copepod biodiversity as an indicator of changes in ocean and climate conditions of the northern California current ecosystem. Limnol. Oceanogr. 51, 2607–2620. https://doi.org/10.4319/lo.2006.51.6.2607.
Ikeda, T., 1985. Metabolic rates of epipelagic marine zooplankton as a function of body mass and temperature. Mar. Biol. 85, 1–11. https://doi.org/10.1007/BF00396409.
Jagadeesan, L., Srinivas, T.N.R., Surendra, A., Kumar, G.S., Aswindev, M.P., Joseph, I., 2020. Copepods size structure in various phases of a cold-core eddy - normalised Abundance Size Spectra (NASS) approach. Continent. Shelf Res. 206, 104197 https://doi.org/10.1016/J.CSR.2020.104197.
Kiørboe, T., 2013. Zooplankton body composition. Limnol. Oceanogr. 58, 1843–1850. https://doi.org/10.4319/LO.2013.58.5.1843.
Krupica, K.L., 2006. Evaluating Size-Based Indices to Monitor Variation in Scotian Shelf Zooplankton Assemblages.
Kwong, L.E., Ross, T., Lüskow, F., Florko, K.R.N., Pakhomov, E.A., 2022. Spatial, seasonal, and climatic variability in mesozooplankton size spectra along a coastal-to-open ocean transect in the subarctic Northeast Pacific. Prog. Oceanogr. 201, 102728 https://doi.org/10.1016/J.POCEAN.2021.102728.
Landeira, J.M., Brochier, T., Mason, E., Lozano-Soldevilla, F., Hernández-León, S., Barton, E.D., 2017. Transport pathways of decapod larvae under intense mesoscale activity in the Canary-African coastal transition zone: implications for population connectivity. Sci. Mar. 81, 299–315.
Lenth, R., Lenth, M.R., 2018. Package 'lsmeans. Am. Statistician 34, 216–221.
Lenz, P.H., Lieberman, B., Cieslak, M.C., Roncalli, V., Hartline, D.K., 2021. Transcriptomics and metatranscriptomics in zooplankton: wave of the future? J. Plankton Res. 43, 3–9. https://doi.org/10.1093/plankt/fbaa058.
Li, K., Ke, Z., Tan, Y., 2018. Zooplankton in the Huangyan Atoll, South China Sea: a comparison of community structure between the lagoon and seaward reef slope. J. Oceanol. Limnol. 36, 1671–1680.
Liu, G., Liu, Z., Gu, B., Smoak, J.M., Zhang, Z., 2014. How important are trophic state, macrophyte and fish population effects on cladoceran community? A study in Lake Erhai. Hydrobiologia 736, 189–204. https://doi.org/10.1007/S10750-014-1906-5/TABLES/3.
Lomartire, S., Marques, J.C., Gonçalves, A.M.M., 2021. The key role of zooplankton in ecosystem services: a perspective of interaction between zooplankton and fish recruitment. Ecol. Indicat. 129, 107867 https://doi.org/10.1016/J.ECOLIND.2021.107867.
Lowry, O.H., Rosebrough, N.J., Farr, A.L., Randall, R.J., 1951. Protein measurement with the Folin phenol reagent. J. Biol. Chem. 193, 265–275.
Maas, A.E., Gossner, H., Smith, M.J., Blanco-Bercial, L., 2021. Use of optical imaging datasets to assess biogeochemical contributions of the mesozooplankton. J. Plankton Res. 43, 475–491. https://doi.org/10.1093/PLANKT/FBAB037.
Mackas, D.L., Greve, W., Edwards, M., Chiba, S., Tadokoro, K., Eloire, D., Mazzocchi, M. G., Batten, S., Richardson, A.J., Johnson, C., Head, E., Conversi, A., Peluso, T., 2012. Changing zooplankton seasonality in a changing ocean: comparing time series of zooplankton phenology. Prog. Oceanogr. 97 (100), 31–62. https://doi.org/10.1016/j.pocean.2011.11.005.
Manríquez, K., Escribano, R., Riquelme-Bugueño, R., 2012. Spatial structure of the zooplankton community in the coastal upwelling system off central-southern Chile in spring 2004 as assessed by automated image analysis. Prog. Oceanogr. 92–95, 121–133. https://doi.org/10.1016/j.pocean.2011.07.020.
Marcolin, C.R., Gaeta, S., Lopes, R.M., 2015. Seasonal and interannual variability of zooplankton vertical distribution and biomass size spectra off Ubatuba, Brazil. J. Plankton Res. 37, 808–819. https://doi.org/10.1093/PLANKT/FBV035.
Medellín-Mora, J., Atkinson, A., Escribano, R., 2020. Community structured production of zooplankton in the eastern boundary upwelling system off central/southern Chile (2003-2012). ICES J. Mar. Sci. 77, 419–435. https://doi.org/10.1093/icesjms/fsz193.
Moyano, M., Rodríguez, J.M., Hernández-León, S., 2009. Larval fish abundance and distribution during the late winter bloom off Gran Canaria Island, Canary Islands. Fish. Oceanogr. 18, 51–61. https://doi.org/10.1111/J.1365-2419.2008.00496.X.
Naito, A., Abe, Y., Matsuno, K., Nishizawa, B., Kanna, N., Sugiyama, S., Yamaguchi, A., 2019. Surface zooplankton size and taxonomic composition in Bowdoin Fjord, northwestern Greenland: a comparison of ZooScan, OPC and microscopic analyses. Pol. Sci. 19, 120–129. https://doi.org/10.1016/J.POLAR.2019.01.001.
Neuer, S., Cianca, A., Helmke, P., Freudenthal, T., Davenport, R., Meggers, H., Knoll, M., Santana-Casiano, J.M., González-Davila, M., Rueda, M.J., Llinás, O., 2007. Biogeochemistry and hydrography in the eastern subtropical North Atlantic gyre. Results from the European time-series station ESTOC. Prog. Oceanogr. 72, 1–29. https://doi.org/10.1016/j.pocean.2006.08.001.
Noji, T.T., 1991. The Influence of Macrozooplankton on Vertical Particulate Flux, pp. 1–9. https://doi.org/10.1080/00364827.1991.10413459 76.
Noyon, M., Poulton, A.J., Asdar, S., Weitz, R., Giering, S.L.C., 2022. Mesozooplankton community distribution on the Agulhas Bank in autumn: size structure and production. Deep Sea Res. Part II Top. Stud. Oceanogr. 195, 105015 https://doi.org/10.1016/J.DSR2.2021.105015.
Ohman, M.D., Romagnan, J.B., 2016. Nonlinear effects of body size and optical attenuation on Diel Vertical Migration by zooplankton. Limnol. Oceanogr. 61, 765–770. https://doi.org/10.1002/LNO.10251.
Oksana, G., Viacheslav, V., 2012. Composition and structure of the zooplankton in coastal waters of Mauritania in winter. J. Sib. Fed. Univ. Biol. 5, 136–150. https://doi.org/10.17516/1997-1389-0141.
Peters, R.H., Wassenberg, K., 1983. The effect of body size on animal abundance. Oecologia 60, 89–96. https://doi.org/10.1007/BF00379325.
Picheral, M., Colin, S., Irisson, J.O., 2017. EcoTaxa, a Tool for the Taxonomic Classification of Images.
Pitois, S.G., Graves, C.A., Close, H., Lynam, C., Scott, J., Tilbury, J., van der Kooij, J., Culverhouse, P., 2021. A first approach to build and test the Copepod Mean Size and Total Abundance (CMSTA) ecological indicator using in-situ size measurements from the Plankton Imager (PI). Ecol. Indicat. 123, 107307 https://doi.org/10.1016/J.ECOLIND.2020.107307.
Platt, T., Denman, K., 1978. The structure of pelagic marine ecosystems. Rapp. Proces Verbaux des Reun.
Platt, T., Denman, K., 1977. Organisation in the pelagic ecosystem. Helgoländer wissenschaftliche Meeresuntersuchungen 1977 301 30, 575–581. https://doi.org/10.1007/BF02207862.
Postel, L., 1990. PhD Thesis. Die Reaktion des Mesozooplanktons, speziell der Biomasse, aufkuÅNstennahen Auftriebvor West afrika, vol. 127. InstitutfuÅN r Meereskunde, Warn.
Quinones, R.A., Platt, T., Rodríguez, J., 2003. Patterns of biomass-size spectra from oligotrophic waters of the Northwest Atlantic. Prog. Oceanogr. 57, 405–427. https://doi.org/10.1016/S0079-6611(03)00108-3.
R Core Team, 2022. R: A Language and Environment for Statistical Computing.
Reyes-Mendoza, O., Herrera-Silveira, J., Mariño-Tapia, I., Enriquez, C., Largier, J.L., 2019. Phytoplankton blooms associated with upwelling at Cabo Catoche. Continent. Shelf Res. 174, 118–131. https://doi.org/10.1016/j.csr.2018.12.015.
Rodriguez, J., Mullin, M.M., 1986. Diel and interannual variation of size distribution of oceanic zooplanktonic biomass. Ecology 67, 215–222. https://doi.org/10.2307/1938521.
Rodríguez, J.M., Hernández-León, S., Barton, E.D., 1999. Mesoscale distribution of fish larvae in relation to an upwelling filament off Northwest Africa. Deep. Res. Part I Oceanogr. Res. Pap. 46, 1969–1984. https://doi.org/10.1016/S0967-0637(99)00036-9.
Rutter, W.J., Kemp, J.D., Bradshaw, W.S., Clark, W.R., Ronzio, R.A., Sanders, T.G., 1968. Regulation of specific protein synthesis in cytodifferentiation. J. Cell. Physiol. 72, 1–18. https://doi.org/10.1002/jcp.1040720403.
San Martin, E., Harris, R.P., Irigoien, X., 2006. Latitudinal variation in plankton size spectra in the Atlantic Ocean. Deep. Res. Part II Top. Stud. Oceanogr. 53, 1560–1572. https://doi.org/10.1016/J.DSR2.2006.05.006.
Schlitzer, R., 2015. Ocean Data View.
Schmoker, C., Arístegui, J., Hernández-León, S., 2012. Planktonic biomass variability during a late winter bloom in the subtropical waters off the Canary Islands. J. Mar. Syst. 95, 24–31. https://doi.org/10.1016/j.jmarsys.2012.01.008.
Schmoker, C., Hernández-León, S., 2013. Stratification effects on the plankton of the subtropical Canary Current. Prog. Oceanogr. 119, 24–31. https://doi.org/10.1016/J.POCEAN.2013.08.006.
Sheldon, R.W., Prakash, A., Sutcliffe, W.H., 1972. The size distribution of particles in the ocean. Limnol. Oceanogr. 17, 327–340. https://doi.org/10.4319/LO.1972.17.3.0327.
Shi, Y., Wang, J., Zuo, T., Shan, X., Jin, X., Sun, J., Yuan, W., Pakhomov, E.A., 2020. Seasonal changes in zooplankton community structure and distribution pattern in the yellow sea, China. Front. Mar. Sci. 7, 391. https://doi.org/10.3389/FMARS.2020.00391/BIBTEX.
Sourisseau, M., Carlotti, F., 2006. Spatial distribution of zooplankton size spectra on the French continental shelf of the Bay of Biscay during spring 2000 and 2001. J. Geophys. Res. 111, 5–9. https://doi.org/10.1029/2005JC003063.
Sprules, W.G., Barth, L.E., 2016. Surfing the biomass size spectrum: some remarks on history, theory, and application. Can. J. Fish. Aquat. Sci. 73, 477–495. https://doi.org/10.1139/CJFAS-2015-0115/ASSET/IMAGES/LARGE/CJFAS-2015-0115F14.JPEG.
Sprules, W.G., Munawar, M., 1986. Plankton Size Spectra in Relation to Ecosystem Productivity, Size, and Perturbation, pp. 1789–1794. https://doi.org/10.1139/f86-222 43, 10.1139/F86-222.
Stemmann, L., Boss, E., 2012. Plankton and particle size and packaging: from determining optical properties to driving the biological pump. Ann. Rev. Mar. Sci 4, 263–290.
Sun, D., Chen, Y., Feng, Y., Liu, Z., Peng, X., Cai, Y., Yu, P., Wang, C., 2021. Seasonal variation in size diversity: explaining the spatial mismatch between phytoplankton and mesozooplankton in fishing grounds of the East China Sea. Ecol. Indicat. 131, 108201 https://doi.org/10.1016/J.ECOLIND.2021.108201.
Suthers, I.M., Taggart, C.T., Rissik, D., Baird, M.E., 2006. Day and night ichthyoplankton assemblages and zooplankton biomass size spectrum in a deep ocean island wake. Mar. Ecol. Prog. Ser. 322, 225–238. https://doi.org/10.3354/MEPS322225.
Thiebaux, M.L., Dickie, L.M., 2011. Structure of the Body-Size Spectrum of the Biomass in Aquatic Ecosystems: A Consequence of Allometry in Predator–Prey Interactions, pp. 1308–1317. https://doi.org/10.1139/f93-148 50, 10.1139/F93-148.
UNESCO, 1968. Zooplankton Sampling. Symposium on the Hydrodynamics of Zooplankton Sampling. Unesco.
Valdés, L., Déniz-González, I., 2015. Oceanographic and biological features in the Canary Current Large Marine Ecosystem.
Vandromme, P., Lars, S., Garcìa-Comas, C., Berline, L., Sun, X., Gorsky, G., 2012. Assessing biases in computing size spectra of automatically classified zooplankton from imaging systems: a case study with the ZooScan integrated system. Methods Oceanogr. 1–2, 3–21. https://doi.org/10.1016/J.MIO.2012.06.001.
Vanni, M.J., Findlay, D.L., 1990. Trophic cascades and phytoplankton community structure. Ecology 71, 921–937.
Wang, W., Sun, S., Sun, X., Zhang, G., Zhang, F., 2020. Spatial patterns of zooplankton size structure in relation to environmental factors in Jiaozhou Bay, South Yellow Sea. Mar. Pollut. Bull. 150, 110698 https://doi.org/10.1016/J.MARPOLBUL.2019.110698.

Woodward, G., Ebenman, B., Emmerson, M., Montoya, J.M., Olesen, J.M., Valido, A., Warren, P.H., 2005. Body size in ecological networks. Trends Ecol. Evol. 20, 402–409.

Woodworth-Jefcoats, P.A., Polovina, J.J., Dunne, J.P., Blanchard, J.L., 2013. Ecosystem size structure response to 21st century climate projection: large fish abundance decreases in the central N orth P acific and increases in the C alifornia C urrent. Global Change Biol. 19, 724–733.

Ye, L., Chang, C.Y., García-Comas, C., Gong, G.C., Hsieh, C. hao, 2013. Increasing zooplankton size diversity enhances the strength of top-down control on phytoplankton through diet niche partitioning. J. Anim. Ecol. 82, 1052–1061. https://doi.org/10.1111/1365-2656.12067.

Yebra, L., Almeida, C., Hernández-León, S., 2005. Vertical distribution of zooplankton and active flux across an anticyclonic eddy in the Canary Island waters. Deep. Res. Part I Oceanogr. Res. Pap. 52, 69–83. https://doi.org/10.1016/j.dsr.2004.08.010.

Zhao, W., Dai, L., Chen, X., Wu, Y., Sun, Y., Zhu, L., 2022. Characteristics of zooplankton community structure and its relationship with environmental factors in the South Yellow Sea. Mar. Pollut. Bull. 176, 113471 https://doi.org/10.1016/J.MARPOLBUL.2022.113471.

Zhou, L., Huang, L., Tan, Y., Lian, X., Li, K., 2014. Size-based Analysis of a Zooplankton Community under the Influence of the Pearl River Plume and Coastal Upwelling in the Northeastern South China Sea, pp. 168–179. https://doi.org/10.1080/17451000.2014.904882.

Zhou, M., 2006. What determines the slope of a plankton biomass spectrum? J. Plankton Res. 28, 437–448. https://doi.org/10.1093/PLANKT/FBI119.